


Article

RELM α Is Induced in Airway Epithelial Cells by Oncostatin M without Requirement of STAT6 or IL-6 in Mouse Lungs In Vivo

Lilian Ho, Ashley Yip, Francis Lao, Fernando Botelho and Carl D. Richards * 

McMaster Immunology Research Centre, Department of Pathology and Molecular Medicine, McMaster University, Hamilton, ON L8P, Canada; hol2@mcmaster.ca (L.H.); yipa1@mcmaster.ca (A.Y.); laof@mcmaster.ca (F.L.); botelhf@mcmaster.ca (F.B.)

* Correspondence: richards@mcmaster.ca; Tel.: +905-525-9140 (ext. 22391)

Received: 26 February 2020; Accepted: 22 May 2020; Published: 27 May 2020



Abstract: Resistin-like molecule alpha (RELM α) and YM-1 are secreted proteins implicated in murine models of alternatively activated macrophage (AA/M2) accumulation and Th2-skewed inflammation. Since the gp130 cytokine Oncostatin M (OSM) induces a Th2-like cytokine and AA/M2 skewed inflammation in mouse lung, we here investigated regulation of RELM α and YM-1. Transient pulmonary overexpression of OSM by Adenovirus vector (AdOSM) markedly induced RELM α and YM-1 protein expression in total lung. In situ hybridization showed that RELM α mRNA was highly induced in airway epithelial cells (AEC) and was co-expressed with CD68 mRNA in some but not all CD68+ cells in parenchyma. IL-6 overexpression (a comparator gp130 cytokine) induced RELM α , but at significantly lower levels. IL-6 (assessing IL-6^{-/-} mice) was not required, nor was STAT6 (IL-4/13 canonical signalling) for AdOSM-induction of RELM α in AEC. AEC responded directly to OSM in vitro as assessed by pSTAT3 activation. RELM α -deficient mice showed similar inflammatory cell infiltration and cytokine responses to wt in response to AdOSM, but showed less accumulation of CD206+ AA/M2 macrophages, reduced induction of extracellular matrix gene mRNAs for COL1A1, COL3A1, MMP13, and TIMP1, and reduced parenchymal alpha smooth muscle actin. Thus, RELM α is regulated by OSM in AEC and contributes to extracellular matrix remodelling in mouse lung.

Keywords: Oncostatin M; RELM α ; airway epithelial cells; lung inflammation

1. Introduction

Chronic respiratory diseases, such as idiopathic pulmonary fibrosis (IPF), chronic obstructive pulmonary disease (COPD), and severe asthma, are conditions that imply a reduction in lung function that involves extracellular matrix (ECM) remodelling [1]. In COPD, damaged alveolar walls and the loss of shape and structure in larger airways reduce gas exchange efficiency [2], whereas IPF and severe asthma are characterized by excessive ECM deposition in the airways or around alveoli, therefore decreasing gas exchange with the capillary network and consequently impairing pulmonary function [1,3,4]. These conditions are often progressive in nature and current therapies have much room for improvement [3,5]. Animal models of lung fibrosis implicate activated T cells and alternatively activated macrophages in the induction of ECM [6,7]. Although cytokines such as transforming growth factor beta (TGF β) [8] and interleukin-4 (IL-4) [9] are critical factors in fibrogenesis in many systems, studies have also shown pathways independent of TGF β /SMAD3 and IL-4/STAT6 that can lead to fibrosis in animal models in vivo [10]. Thus, understanding the various mechanisms of how ECM remodelling occurs and through which cells and signaling molecules will provide a better understanding to inform new potential therapeutic approaches separate from the TGF β pathway.

Several members of the gp130 cytokine family have been implicated in inflammatory responses of chronic respiratory diseases and ECM remodelling in the lung, including Oncostatin M (OSM) and IL-6 [11–14]. OSMR β and gp130 receptor chains, required for the active OSM receptor complex on cell surfaces [12], are widely expressed in stromal/connective tissue cells, including those responsible for ECM remodelling in the lung [15,16]. Although receptors for other gp130 cytokines, such as IL-6R α , may also be expressed on connective tissue cells, their expression are relatively lower than OSMR β [17]. In addition, we have previously shown that OSM is able to activate such cells more robustly than other cytokines in this family [13,18]. Furthermore, OSM has been detected at elevated levels in the broncho-alveolar lavage (BAL) fluid of IPF patients, sputum of asthma and COPD patients, as well as in allergic rhinitis tissue, suggesting that OSM may be participating in the pathogenesis of these chronic diseases [11,19–21]. We have previously shown that overexpression of OSM induces ECM accumulation and accumulation of arginase-1⁺ (Arg1) alternatively activated (AA/M2-like) macrophages, which was associated with eosinophilia and a Th2-like skewed cytokine profile in lungs of C57Bl/6 mice [22]. In preliminary work for the present study, we observed a marked induction of the gene for resistin-like molecule alpha (RELM α), a typical AA/M2 macrophage product. Regulation of RELM α by OSM has not been previously described, and whether RELM α participates in OSM-induced inflammation and pathology is examined here.

RELM α , also known as found in inflammatory zone 1 (FIZZ1), is a member of the RELM/FIZZ family of cysteine-rich secreted proteins that share a highly conserved signature 10-cysteine residues motif in the C-terminal domain [23,24]. RELM α (9.4 kDa) can be secreted by several different cell types including AA/M2 macrophages, eosinophils, B lymphocytes, adipocytes, and alveolar epithelial cells [23,25–28]. In AA/M2 macrophages, RELM α can be up-regulated by IL-4 or IL-13 *in vitro*, and its dependence on STAT6 in such cells was confirmed using STAT6 knockout mice [29,30]. RELM α has been implicated in murine models of experimental asthma, parasitic infection, pulmonary fibrosis, and wound healing [23,26,31–35]. Liu et al. showed that RELM α -deficient mice challenged with bleomycin were protected from the fibrotic phenotype, suggesting a profibrotic role for RELM α [33]. In a different model, Nair et al. demonstrated that RELM α -deficient mice challenged with parasitic infection developed exacerbated lung inflammation associated with elevated Th2 cytokine expression, presenting a healing phenotype [26]. Given the proposed functions of RELM α in mouse lung inflammation, in this study we evaluate the regulation of RELM α by gp130 cytokines OSM and IL-6 *in vivo* and examine the roles of RELM α in OSM-induced lung inflammation and ECM gene expression *in vivo* using RELM α -deficient mice. We show here that OSM is a potent inducer of RELM α in airway epithelial cells, markedly increases RELM α levels locally in lung, and that RELM α contributes to the ECM remodelling processes induced by OSM.

2. Materials and Methods

2.1. Mice and Cell Culture

Female BALB/c wild-type (6–8 weeks old) were purchased from Charles River Laboratories (Wilmington, MA, USA). Female C57Bl/6 wild-type (6–10 weeks old), IL-6^{-/-} (C57Bl/6 background; 6–8 weeks old), and RELM α ^{-/-} mice (C57Bl/6 background; 8–10 weeks old) purchased from The Jackson Laboratory (Bar Harbor, ME, USA) were acclimatized one week prior to experimental procedures, and housed under specific pathogen-free conditions within the McMaster University Central Animal Facility. All experimental procedures were approved by the McMaster University Animal Research Ethics Board. Mice were endo-tracheally administered with sterile PBS or 5×10^7 PFU of AdDel70, AdOSM, or 3×10^7 PFU of AdIL-6. Animals were culled 2, 7, or 14 days following administration.

2.2. Airway Epithelial Cells

C57Bl/6 mouse adult Tracheal-Bronchial Epithelial Cells (TBE cells; Creative Bioarray (cat# CSC-9087J), Shirley, NY, USA) were cultured in SuperCult[®] (Creative Bioarray). Complete Mouse

Epithelial Cell culture basal medium (containing 0.1% insulin-transferin-selenium (ITS), 0.1% epidermal growth factor (EGF), 1% L-glutamine, 1% antibiotic-antimycotic solution and 2% fetal bovine serum). Cells were grown on sterile culture flasks coated with a 1% gelatin solution (Cell Attachment 1 × (cat#S006100) from ThermoFisher Scientific). For cell stimulation, cells were stimulated in complete mouse epithelial cell culture medium for 24 h to 5 days, with 15,000 cells/well in 96-well plates or 50,000 cells/well in 6-well plates.

2.3. Sample Collection and Tissue Processing

Broncho-alveolar lavage (BAL) fluid and cells were recovered from lungs by washing twice with 500 µL of cold sterile PBS. Cells were recovered by centrifugation and enumerated by manual counting using a hemocytometer, then cytocentrifuged and stained with Hema-3 fixative solutions (Thermo Fisher Scientific, Waltham, MA, USA) for differential cell analysis. After BAL collection, the left lobe of lungs was perfused with 10% formalin for 48 h then transferred and stored in 70% ethanol. A section of the right lobe was frozen in liquid nitrogen and stored in -80°C until further processing. Frozen tissue samples were crushed and equal portions were resuspended in radioimmunoprecipitation assay (RIPA) buffer containing protease inhibitors (Aprotinin, PMSF, Na_3VO_4 , DTT) for protein, or Trizol (Thermo Fisher Scientific, Waltham, MA, USA) for RNA extraction. Protein samples were processed using a homogenizer and RNA samples purified by phenol-chloroform extraction. Samples were stored in -80°C until further analysis.

2.4. Histology, Immunohistochemistry and Chromogenic In Situ Hybridization (CISH)

Following formalin fixation, the left lobe of lungs was dissected into three sections per lung, embedded in paraffin and stored at rt for further analysis. Sections of 3 µm were cut and stained with hematoxylin and eosin (H&E) to assess lung pathology and periodic acid-Schiff (PAS) to assess mucous-producing goblet cells. Immunohistochemistry for Ki67 to assess cell proliferation and alpha smooth muscle actin (αSMA) was also performed. Slide images were captured using Zeiss Axio Imager 2, or scanned using Aperio ImageScope. Quantification of Ki67⁺ cells was performed on ImageJ, and quantification of αSMA^+ staining on QuPath. Chromogenic in situ hybridization (CISH) for mouse RELM α , YM-1 and CD68 mRNA was performed using the RNAscope[®] 2.5 Duplex Assay Kit (Advanced Cell Diagnostics, Newark, CA, USA) and stained the BOND Ix automated staining instrument (Leica). Formalin-fixed paraffin-embedded lung tissue sections were pretreated with heat and protease prior to hybridization with the target oligo probes. Specific RNA staining signal was identified as punctate dots.

2.5. Flow Cytometry

Whole lung mononuclear cell suspensions were generated from a section of the right lobe by mechanical mincing and collagenase digestion. Tissues were degraded with Collagenase I and DNase I for 2 h on an incubated shaker at 37 °C. Debris were removed by passage through 45 µm mesh filter and cells were resuspended in 1 × PBS/0.3% bovine serum albumin (BSA). Cells were stimulated with phorbol 12-myristate 13-acetate (PMA) and ionomycin for 4 h prior to flow cytometric analysis. Forward scatter and side scatter parameters and Zombie-Aqua dye (BioLegend, San Diego, CA, USA) were used to define the live cell gate. Cells were stained with Zombie-Aqua dye for 20 min at room temp (RT) prior to surface staining with fluorophore-conjugated antibodies. Cells were surface-stained for 30 min at 4 °C with antibodies for CD3, CD4, CD38, and CD45 (BD Biosciences, San Jose, CA, USA). Following surface staining, cells were fixed with BD Cytofix/CytoPerm (BD Biosciences, San Jose, CA, USA) for 20 min at 4 °C and then washed with BD 1 × Perm/Wash (BD Biosciences, San Jose, CA, USA) prior to intracellular staining for 30 min at 4 °C with antibodies for CD206 and IFN γ (BD Biosciences, San Jose, CA, USA). Cells were then washed and resuspended in 1 × PBS/0.3% BSA for analysis on the BD LSR II flow cytometer.

2.6. Western Blot

BAL fluid or culture supernatants were loaded onto 15% SDS-PAGE gels and separated by electrophoresis at 120 V for 1 h, then transferred to nitrocellulose membranes at 400 mA for 1 h. Blots were blocked using Odyssey Blocking Buffer (LI-COR Biosciences, Lincoln, NE, USA) for 1 h at RT, then probed using rabbit anti-RELM α polyclonal antibody (PeproTech, Rocky Hill, NJ, USA) and goat anti- β -actin polyclonal antibody (Santa Cruz Biotechnology, Dallas, TX, USA) overnight at 4 °C. The following day blots were washed with 1 \times Tris-buffered saline (TBS) + 0.15% Tween20, and anti-rabbit and anti-goat secondary antibodies (LI-COR Biosciences, Lincoln, NE, USA) were added to blots for 45 min at RT. After subsequent washes, blots were imaged using an Odyssey LI-COR Imaging System.

2.7. Reverse Transcription Polymerase Chain Reaction (RT-PCR) / NanoString

Lung RNA purified by phenol-chloroform extraction were reverse transcribed into cDNA and stored at -80 °C. cDNA was analyzed by Taqman[®] assay (Applied Biosystems, Foster City, CA, USA) using pre-determined assay reagents and specific probes for RELM α and 18S. Gene expression was also measured by NanoString Technologies (Seattle, WA, USA). Analysis of raw mRNA counts was performed using nSolver[™] Analysis Software v4.0. Gene expression levels were normalized to housekeeping genes *Actb* and *Pgk1*. Raw Nanostring data are shown, where counts below 10 are considered below the limit of detection.

2.8. Enzyme-Linked Immunosorbent Assay (ELISA)

BAL fluid and serum samples from mice were analyzed using commercially available DuoSet ELISA kits from R&D Systems (Minneapolis, MN, USA) for YM-1 and eotaxin-2. For measuring RELM α by ELISA, an in-house sandwich ELISA was developed using an anti-mouse RELM α polyclonal antibody and a biotinylated anti-mouse RELM α polyclonal antibody (PeproTech, Rocky Hill, NJ, USA).

2.9. Statistical Analysis

Statistical analyses were carried out using GraphPad Prism 7. The Student's t test, one-way or two-way analysis of variance was used to determine significant differences between sample groups, where $*p < 0.05$, $**p < 0.01$, $***p < 0.001$, $****p < 0.0001$.

3. Results

3.1. RELM α is Induced Upon Overexpression of OSM in Lungs of C57Bl/6 Mice and is Highly Expressed in Airway Epithelial Cells

To examine the in vivo regulation of RELM α , C57Bl/6 were endo-tracheally administered with PBS, the empty control vector AdDel70, or AdOSM to induce transient overexpression of mOSM as previous [13,36,37] in the lungs for seven or 14 days. Lung tissues were assessed for RELM α mRNA expression, and BAL fluid and serum were analyzed for RELM α protein. In AdDel70-treated C57Bl/6 mice, RELM α mRNA was detectable at low levels, which was significantly up-regulated upon treatment with AdOSM at day 7 (Figure 1A, left panel). At the protein expression level (as assessed by ELISA), RELM α was detectable at basal levels (~ 100 ng/mL) in BAL fluid of naïve and AdDel70-treated C57Bl/6 mice, and 7 and 14 days following overexpression of OSM, RELM α protein detected was markedly induced ~ 180 -fold to up to approximately 12 μ g/mL at day 7, and afterwards decreased to approximately 4 μ g/mL by day 14 (Figure 1A, middle panel). RELM α was present at 150–200 ng/mL in serum of control animals and elevated upon AdOSM infection at both days 7 and 14 in C57Bl/6 mice (Figure 1A, right panel).

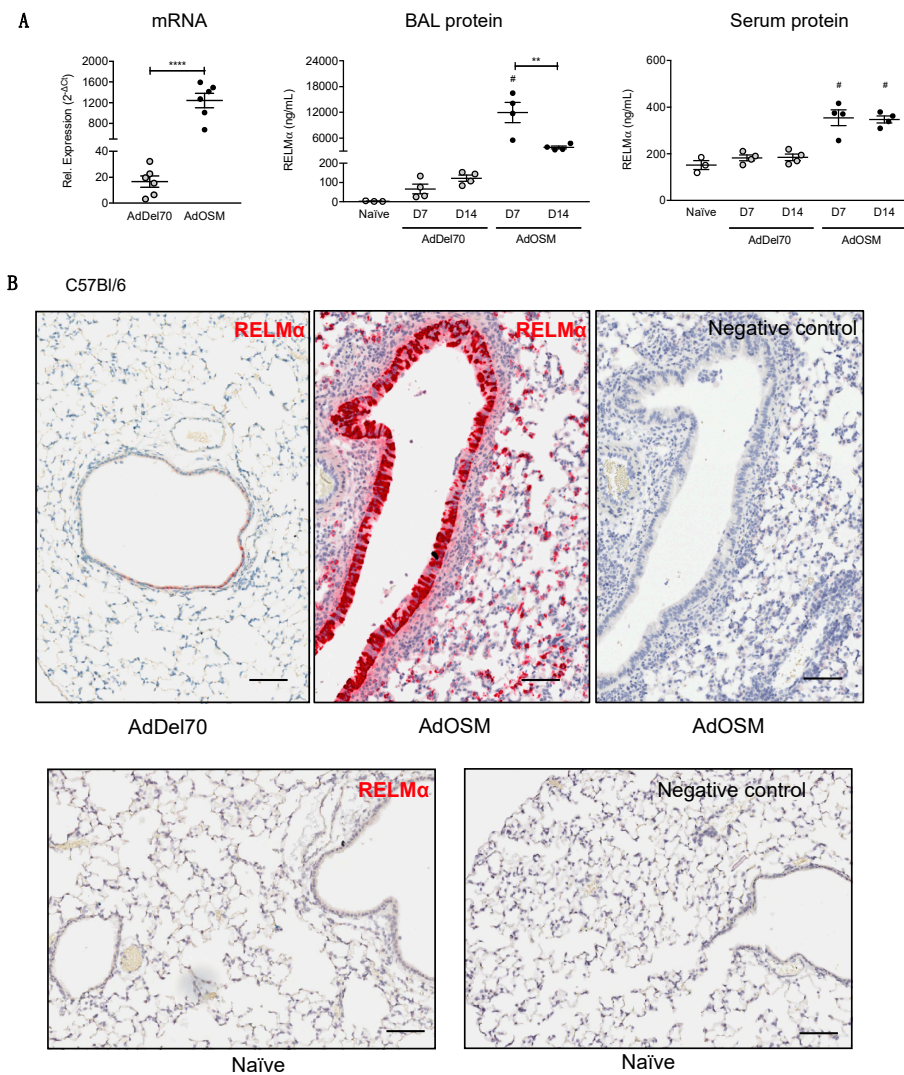


Figure 1. Transient overexpression of OSM induces RELM α mRNA and protein expression in lungs of C57Bl/6 mice. **(A)** RELM α mRNA levels in total lung extracts, 7 days following administration of AdDel70 or AdOSM, and expressed relative to 18S ribosomal RNA. RELM α protein levels in BAL fluid (middle panel) and serum (right panel) 7 and 14 days post-infection (D7, D14) were assessed by ELISA. Data are expressed as mean \pm SEM ($n = 3-6$ mice/group). Statistical significance determined by one-way ANOVA with Tukey's post hoc test ($\# p < 0.05$ relative to controls at the indicated time point; $** p < 0.01$, $**** p < 0.0001$ between indicated groups). **(B)** Chromogenic in situ hybridization (CISH) of mouse lung sections at day 7 of AdDel70 (top left panel) or AdOSM (top middle panel) using specific RELM α probe. The top right panel shows a serial section adjacent to the middle panel processed without the RELM α probe. Bottom panels show naïve lung sections with RELM α probe (left) or no probe (right). Scale bars, 50 μ m.

Given that previous studies have shown that RELM α can be expressed in other cell types in addition to AA/M2 macrophages [26,38], we sought to determine the cell sources of RELM α following AdOSM treatment. Lung tissue sections from C57Bl/6 wild-type were analyzed for mRNA by chromogenic in situ hybridization (CISH) to identify mRNA signals (Figures 1B and 2). In naïve and AdDel70-treated lungs, RELM α was expressed in few cells of the airway epithelium. Upon overexpression of OSM for seven days, RELM α was highly expressed in columnar airway epithelial cells and was also expressed in mononuclear cells throughout the lung parenchyma (Figure 1B). Lung tissue sections (Day 7 after treatment) were further analyzed by co-stain for RELM α and CD68 (a marker of macrophages) in Figure 2. There was no detectable CISH staining for RELM α in RELM α^{-} -deficient

lungs as expected (Figure 2A lower panels). CD68⁺ RELM α ⁻ cells were found throughout the parenchyma across all treatments. In the lung parenchyma of AdOSM-treated wild-type mice, CD68⁺/RELM α ⁺ macrophages were also observed, as demonstrated by co-localization of both stains (Figure 2B, left panel), however many cells in the parenchyma did not co-localize RELM α and CD68, while RELM α was strongly positive in airway epithelial cells (upper portion of 2A upper right panel). To determine if airway epithelial cells can respond to OSM directly, we assessed cell signaling response of primary mouse airway epithelial cells to OSM and other cytokines (Figure 2C). These cultures responded robustly with phospho-STAT3 elevation to OSM, to a low extent to IL-6, but not other gp130 cytokines LIF or IL-31, or to IL-4. Full blots are shown in Supplementary Materials, Figure S1.

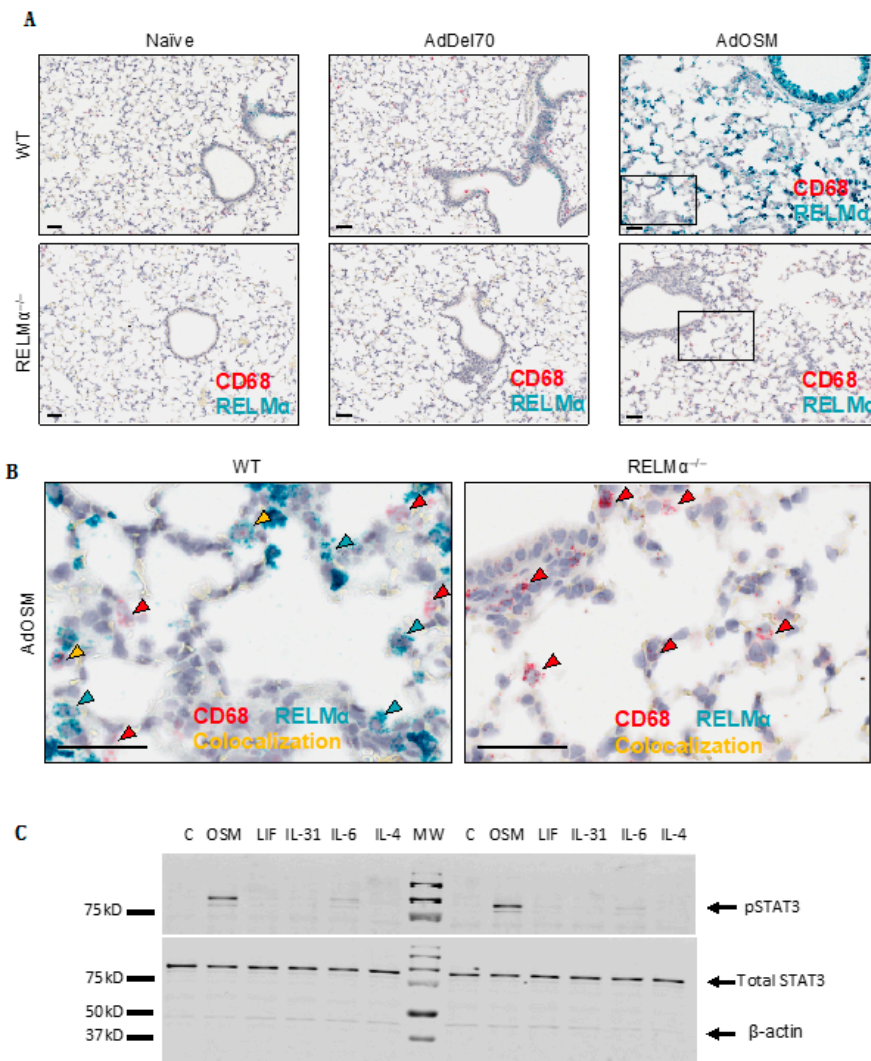


Figure 2. RELM α mRNA is highly induced in columnar airway epithelial cells. (A) Representative images ($n = 5$ mice/group) are shown of CISH staining for RELM α (green-blue) and CD68 (red, a macrophage marker) in formalin-fixed paraffin-embedded lung tissue sections from naive, AdDel70- or AdOSM-treated at day 7 as indicated in wild-type (upper panels) or RELM α ^{-/-} mice (lower panels). Scale bars, 50 μ m. (B) High magnification images of indicated regions (boxed) from AdOSM-treated mouse lungs from right panels of (A) RELM α (green-blue) and CD68 (red) mRNA signals show as punctate dots unless at very high levels in which signals converge. Scale bars, 50 μ m. Co-localization of both signals is indicated as yellow arrowheads in wild-type mice. (C) C57Bl/6-derived murine airway epithelial cells were stimulated in vitro for 1 h with 20ng/ml of OSM, leukemia inhibitory factor (LIF), IL-31, IL-6 or IL-4 and whole cell extracts probed for phospho-STAT3 (pSTAT3), total STAT3 and β -Actin by Western Blotting. Two separate cell culture experiments are shown.

3.2. IL-6 and STAT3 are not Required for Airway Epithelial Cell Responses to OSM

As a comparator of OSM activity to the prototypical gp130 cytokine IL-6, AdIL-6 was administered to C57Bl/6 mice to induce transient overexpression of mouse IL-6 for two and seven days and compared to mice treated in parallel with AdOSM. RELM α in BAL fluid quantified by ELISA (Figure 3A, left panel) showed a similar trend in that AdIL-6 induced RELM α but to markedly lower levels than AdOSM (2 vs 6 $\mu\text{g}/\text{mL}$ at Day 7), and where RELM α levels at day 2 appeared elevated but not statistically different from controls. Western blots (right panels of Figure 3A–C) of whole lung extracts showed that a full length, single band was detected at the expected molecular weight (~ 10 kDa), and reflected the observations found in BAL. An example of full blots probed for RELM α with recombinant RELM α as a comparator for size and amount is depicted in Figure S2.

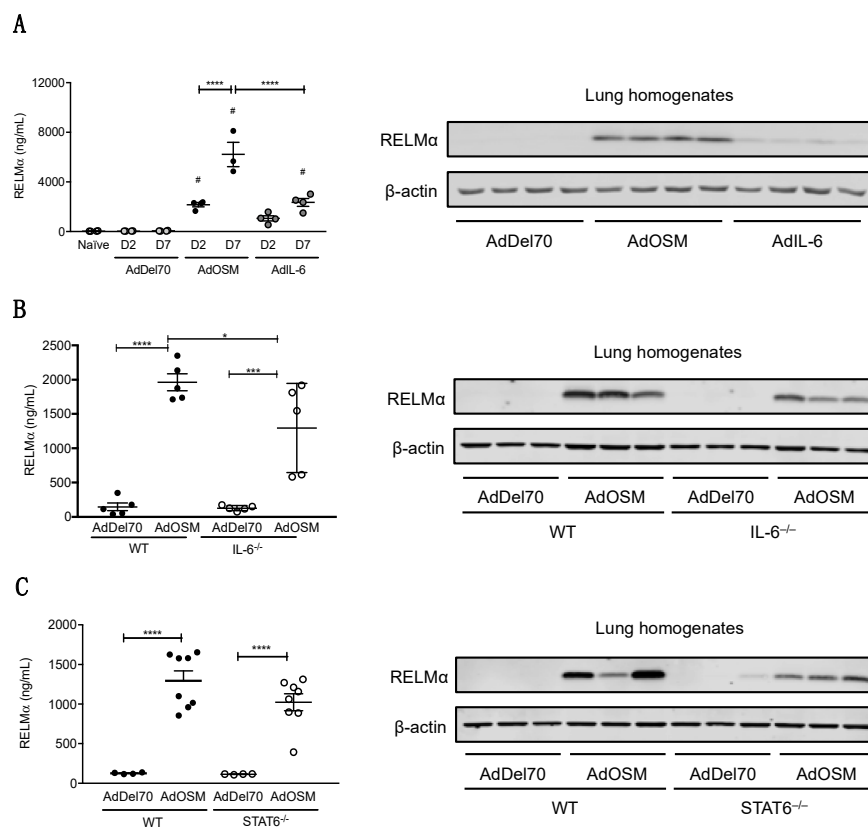


Figure 3. Induction of RELM α by OSM in whole lung IL-6 $^{-/-}$ and STAT6 $^{-/-}$ mice. (A) RELM α protein levels in BAL fluid from C57Bl/6 mice at day 2 or day 7 after AdDel70, AdOSM or AdIL-6 treatment, as assessed by ELISA (left panel). Total lung homogenates from separate C57Bl/6 mice 7 days post-infection were analyzed by Western blot for RELM α (right panel, 4 separate mice/group). (B) Total lung homogenates from wild-type and IL-6 $^{-/-}$ C57Bl/6 mice 7 days post-infection were analyzed by ELISA (left panel) and Western blot (3 separate mice/group, right panel) for RELM α protein levels. (C) Total lung homogenates from wild-type and STAT6 $^{-/-}$ C57Bl/6 mice 7 days post-infection were analyzed by ELISA (left panel) and Western blot (3 separate mice/group, right panel) for RELM α . Data for ELISAs (left panels) are expressed as mean \pm SEM ($n = 4$ –8 mice/group). Statistical significance was determined by one-way or two-way ANOVA with Tukey's post hoc test (# $p < 0.05$ relative to controls at the indicated time point; * $p < 0.05$, *** $p < 0.001$, **** $p < 0.0001$ between indicated groups).

To determine if IL-6 is required for AdOSM-induced RELM α expression, wild-type C57Bl/6 and IL-6 $^{-/-}$ mice were administered AdDel70 or AdOSM, and whole lung extracts were assessed for RELM α by ELISA (Figure 3B, left panels). In these assays of whole lung extracts, RELM α was low/non-detectable in AdDel70-treated lungs, and elevated significantly by AdOSM in wt or IL-6 $^{-/-}$ mice (Figure 3A,B), suggesting the IL-6 was not required for total lung RELM α protein load. Since skewing of macrophages

populations toward AA/M2 phenotypes involves signals induced by IL-4/IL-13 and STAT6 conical signaling, we assessed the level of RELM α in STAT6 $^{-/-}$ mice. Total lung RELM α levels induced by AdOSM were not significantly reduced in STAT6 $^{-/-}$ mice (Figure 3C). CISH staining for RELM α mRNA in lung tissue sections of both IL-6 $^{-/-}$ and STAT6 $^{-/-}$ animals are shown in Figure 4. There was no detectable staining in sections processed without a specific probe for RELM α (Figure S3A,B). In either strain of IL-6 $^{-/-}$ or STAT6 $^{-/-}$ mouse lungs, AdOSM induced RELM α mRNA in the lung airway epithelial cells, suggesting no absolute requirement of either of these pathways for OSM induction of these cells. There was minimal change qualitatively in IL-6 $^{-/-}$ mouse lung parenchymal RELM α mRNA signals (Figure 4A,B), but a clear qualitative decrease in RELM α mRNA signals in the parenchymal cells in STAT6 $^{-/-}$ mouse lung sections (Figure 4C,D).

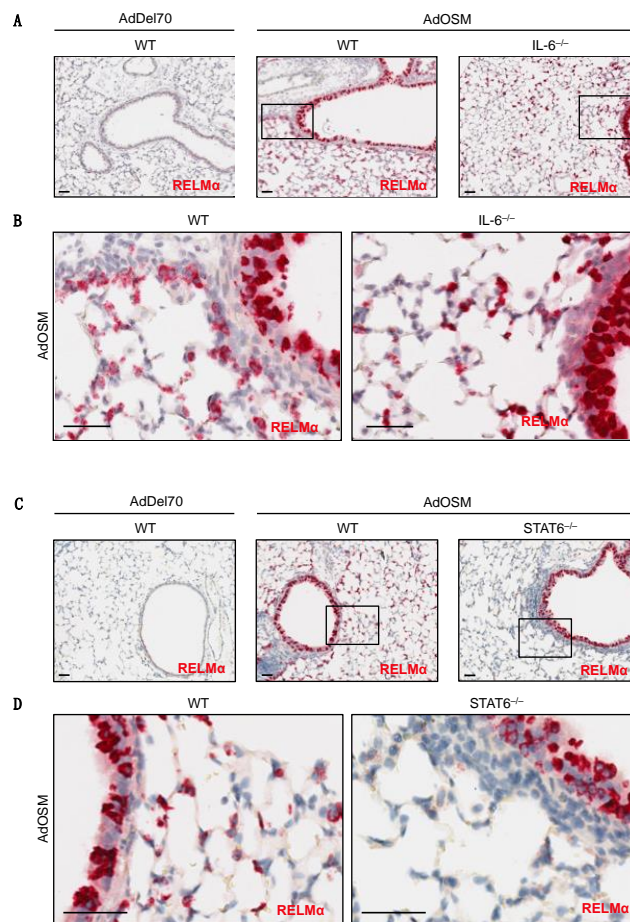


Figure 4. RELM α mRNA induction in situ by OSM in IL-6 $^{-/-}$ and STAT6 $^{-/-}$ mice. Representative images are shown of CISH staining for RELM α (red) in formalin-fixed paraffin-embedded lung tissue sections from C57Bl/6 mice 7 days after treatment ($n = 4-8$ mice/group). (A) RELM α mRNA (red) in AdDel70-treated wild-type, AdOSM-treated wild-type or IL-6 $^{-/-}$ mouse lung sections as indicated. (B) High magnification images of boxed regions in A from AdOSM-treated mouse lungs of wild-type (left panel) or IL-6 $^{-/-}$ (right panel). (C) RELM α mRNA (red) in AdDel70-treated wild-type, AdOSM-treated wild-type and STAT6 $^{-/-}$ mouse lung sections as indicated. (D) Higher magnification images of indicated (boxed) regions from AdOSM-treated mouse lungs in (C). Scale bars, 50 μ m.

3.3. YM-1 Is Induced by AdOSM

Since YM-1 is another well-recognized secreted product and marker of AA/M2 macrophages, we also assessed the expression of YM-1 in the AdOSM model. Figure 5A (left panel) shows that AdOSM but not AdIL-6 elevated YM-1 protein was found in whole lung extracts, and this was significantly reduced in IL-6 $^{-/-}$ whole lung extracts (Figure 5A middle panel) but not in STAT6 $^{-/-}$ mice

(right panel). To determine which cells express YM-1 in this system, we completed CISH analysis staining for YM-1 mRNA (green-blue) and OSM mRNA (red) on tissue sections of AdDel70 and AdOSM treated mouse lungs (Figure 5B,C). YM-1 mRNA+ cells were markedly increased in the parenchyma of AdOSM treated animals compared to AdDel70, and primarily localized to mononuclear cells. Interestingly, YM-1 mRNA signal was also evident in the airway epithelial cells of AdOSM treated mice, although not as prominent as RELM α (Figures 1 and 2). Strong OSM mRNA signals were observed in some of the airway epithelial cells, reflecting the vector-encoded OSM mRNA and the well-established cell tropism of Adenovirus constructs for these cells. There was no evidence of staining in sections using the detection systems without specific probe for YM-1 or OSM (Figure S3C), either in the parenchyma or the airway epithelium (both regions are shown in the control section).

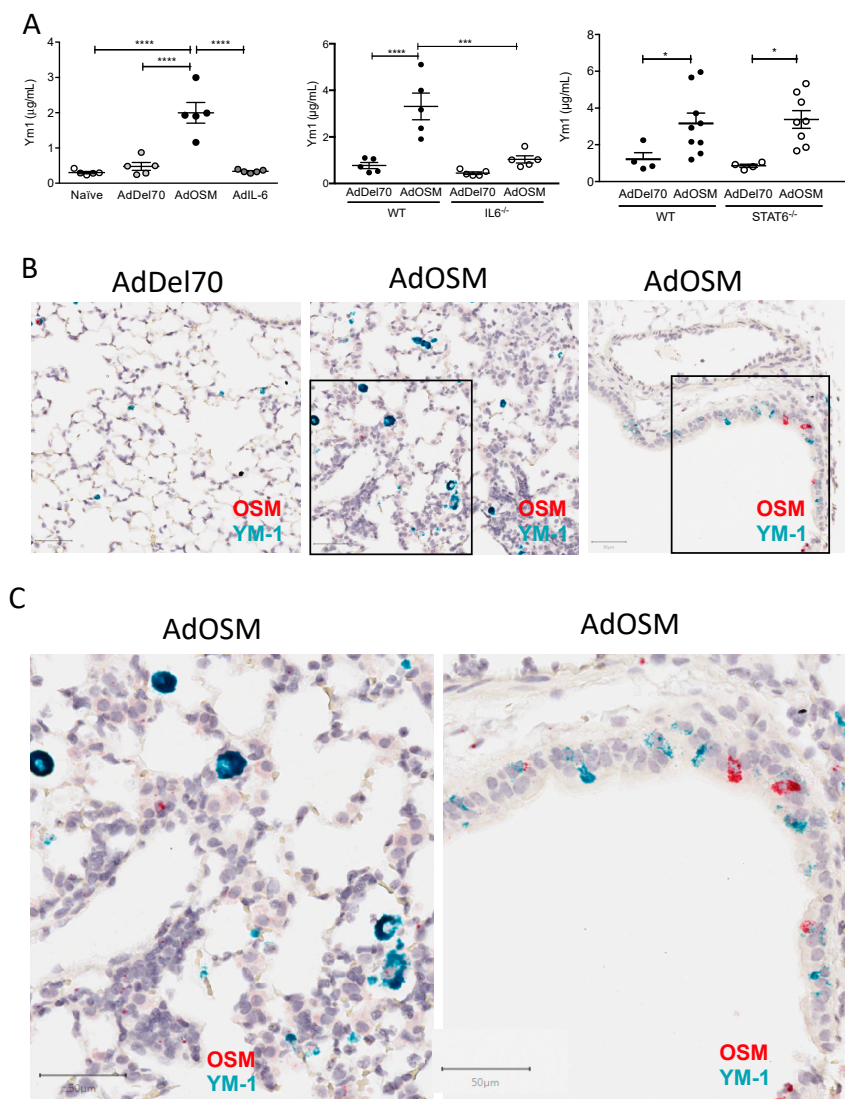


Figure 5. Induction of total lung YM-1 protein and YM-1 mRNA in situ by AdOSM. **(A)** YM-1 protein levels in total lung homogenates at day 7 post-treatment with AdDel70, AdOSM or AdIL-6 in wild-type, IL-6^{-/-} or STAT6^{-/-} mice (as indicated) assessed by ELISA. Data are expressed as mean ± SEM ($n = 4-6$ mice/group). Statistical significance determined by one-way ANOVA with Tukey's post hoc test (left panel) or by two-way ANOVA with Bonferroni's post hoc test (right panels) (* $p < 0.05$, *** $p < 0.001$, **** $p < 0.0001$ between indicated groups). **(B)** Representative images are shown of CISH for YM-1 (green-blue) and OSM (red) in formalin-fixed paraffin-embedded lung tissue sections from mice 7 days after treatments as indicated. **(C)** Higher magnification images of boxed regions in B from AdOSM-treated mouse lungs of wild-type mice. Scale bars, 50 μm .

3.4. RELM α Supports Maximal CD206⁺ M2 Macrophage Numbers Induced by AdOSM

Although RELM α has been implicated in several different murine models of allergic inflammation, pulmonary fibrosis, and helminth infection, its role in type 2 inflammation in the lung is not fully understood. To investigate functions of RELM α in OSM-mediated lung inflammation, wild-type and RELM $\alpha^{-/-}$ mice were endo-tracheally administered PBS, AdDel70, or AdOSM for 7 days, and BAL fluid and lung tissue were examined. RELM α mRNA in naive or AdOSM-induced lungs was non-detectable in RELM $\alpha^{-/-}$ mice, as assessed by Nanostring analysis of RNA extracted from whole lung tissue (Figure 6A, left panel), nor was RELM α protein detectable by ELISA of the BAL fluid (Figure 6B) or as assessed in Western blot analysis of whole lung homogenates of RELM $\alpha^{-/-}$ mice (Figure 6C). OSM mRNA in whole lung and protein in BAL fluid were also measured to compare overexpression of the cytokine in AdOSM-treated animals. The absence of RELM α did not affect the overexpression of Adenovirus-encoded OSM mRNA or protein in whole lung or BAL fluid as assessed by Nanostring or ELISA (Figure 6A,B, right panels). Analysis of Eotaxin-2, previously shown to be induced by AdOSM (22), and YM-1 protein in BAL showed robust elevation by AdOSM and induction was not altered in RELM $\alpha^{-/-}$ mice (Figure 6B lower panels). Consistent with previous findings [22], AdOSM-treated wild-type mice demonstrated accumulation of eosinophils, lymphocytes, and neutrophils in BAL fluid in comparison to control animals. RELM α -deficiency did not appreciably affect the accumulation of these inflammatory cell populations detected at day 7 in BAL (Figure 7A).

We next examined whether RELM α would affect the accumulation of AA/M2 macrophages in lungs treated with AdOSM by flow cytometry (Figure 7B). Macrophages were classified as CD45⁺ (hematopoietic cell marker), F4/80⁺ (macrophage marker), and either CD206⁺ (AA/M2 macrophage marker) or CD38⁺ (M1 macrophage marker). Similar to previous observations [22], AdOSM induced the accumulation of CD206⁺ CD38⁻ AA/M2 macrophages in the lung at day 7, and CD38⁺ CD206⁻ M1 macrophages also accumulated in the lung (Figure 7B). In the absence of RELM α , there was approximately 60% reduction in total numbers of CD206⁺ AA/M2 macrophages in the AdOSM group in comparison to wild-type counterparts, whereas there was no significant effect of RELM α -deficiency on CD38⁺ M1 macrophage detection. Th1 cells were also identified through flow cytometry as CD45⁺, CD3⁺ (T cell marker), CD4⁺ (T helper cell marker), and IFN γ ⁺ (Th1 cell marker). At day 7, AdOSM markedly induced the accumulation of IFN γ -producing Th1 cells in the lungs of both wild-type and RELM $\alpha^{-/-}$ mice, with 40% fewer total IFN γ ⁺ Th1 cells in knockout animals in comparison to wild-types (Figure 7C). Thus, OSM-induced lung inflammation and accumulation of AA/M2 and Th1 cells may be regulated in part through RELM α .

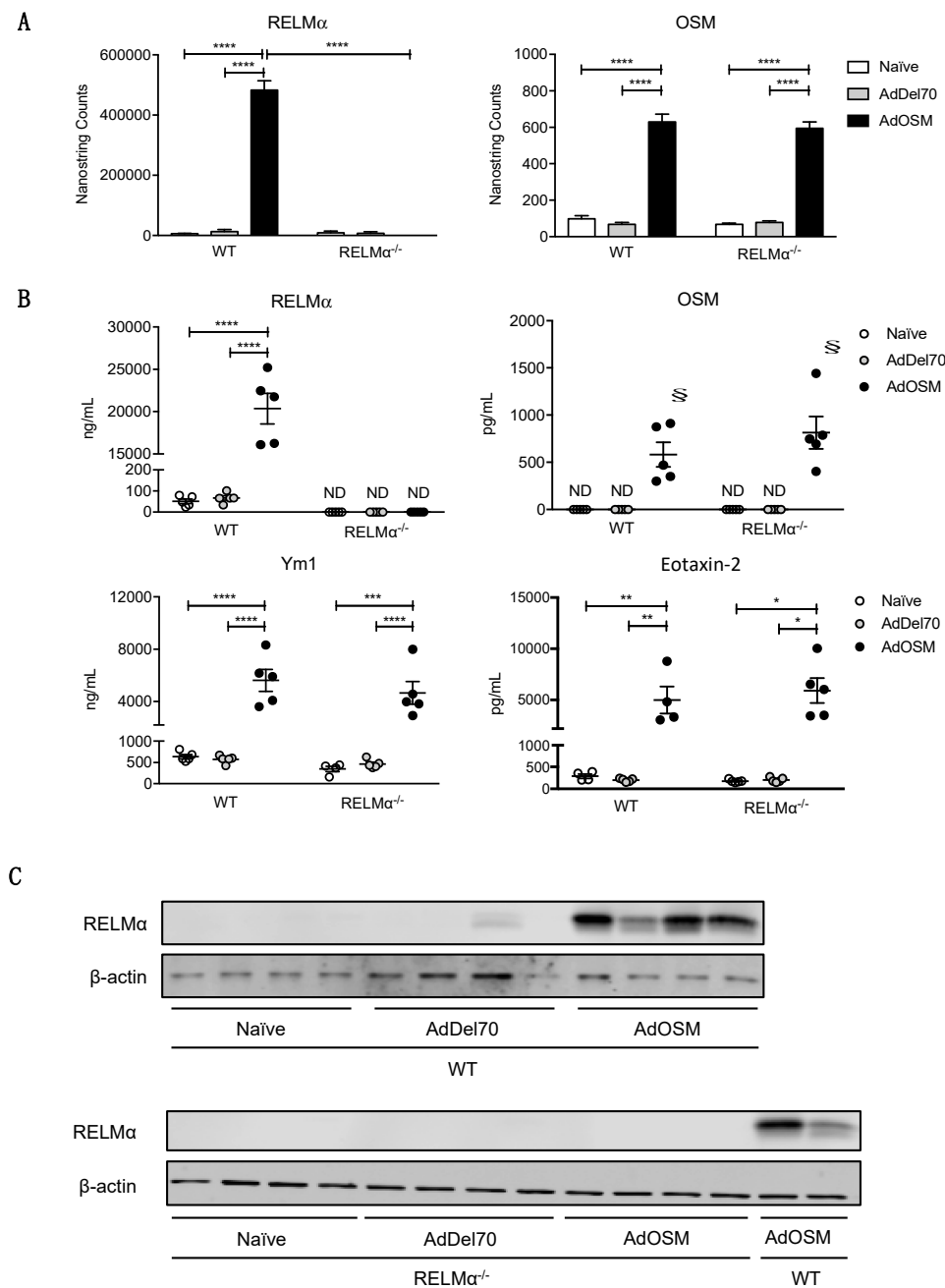


Figure 6. RELM α -deficiency does not alter OSM, Eotaxin-2 or YM-1 levels induced by AdOSM vector. **(A)** Total lung mRNA expression of RELM α (left panel) and OSM (right panel) analyzed by NanoString technology. Gene expression levels are normalized to housekeeping genes ACTB and PGK1. **(B)** RELM α , OSM, Eotaxin-2 and YM-1 protein in BAL fluid were quantified by ELISA. Data **(A,B)** are expressed as mean \pm SEM ($n = 5$ mice/group). Statistical significance was determined by two-way ANOVA with Tukey's post hoc test (* $p < 0.05$, ** $p < 0.01$, *** $p < 0.001$, **** $p < 0.0001$ between indicated groups; § $p < 0.05$ relative to the limit of detection of the assay). **(C)** Total lung homogenates (4 separate animals/group) were probed by Western blot for RELM α and β -actin protein expression in individual wt or RELM $\alpha^{-/-}$ mice treated as indicated.

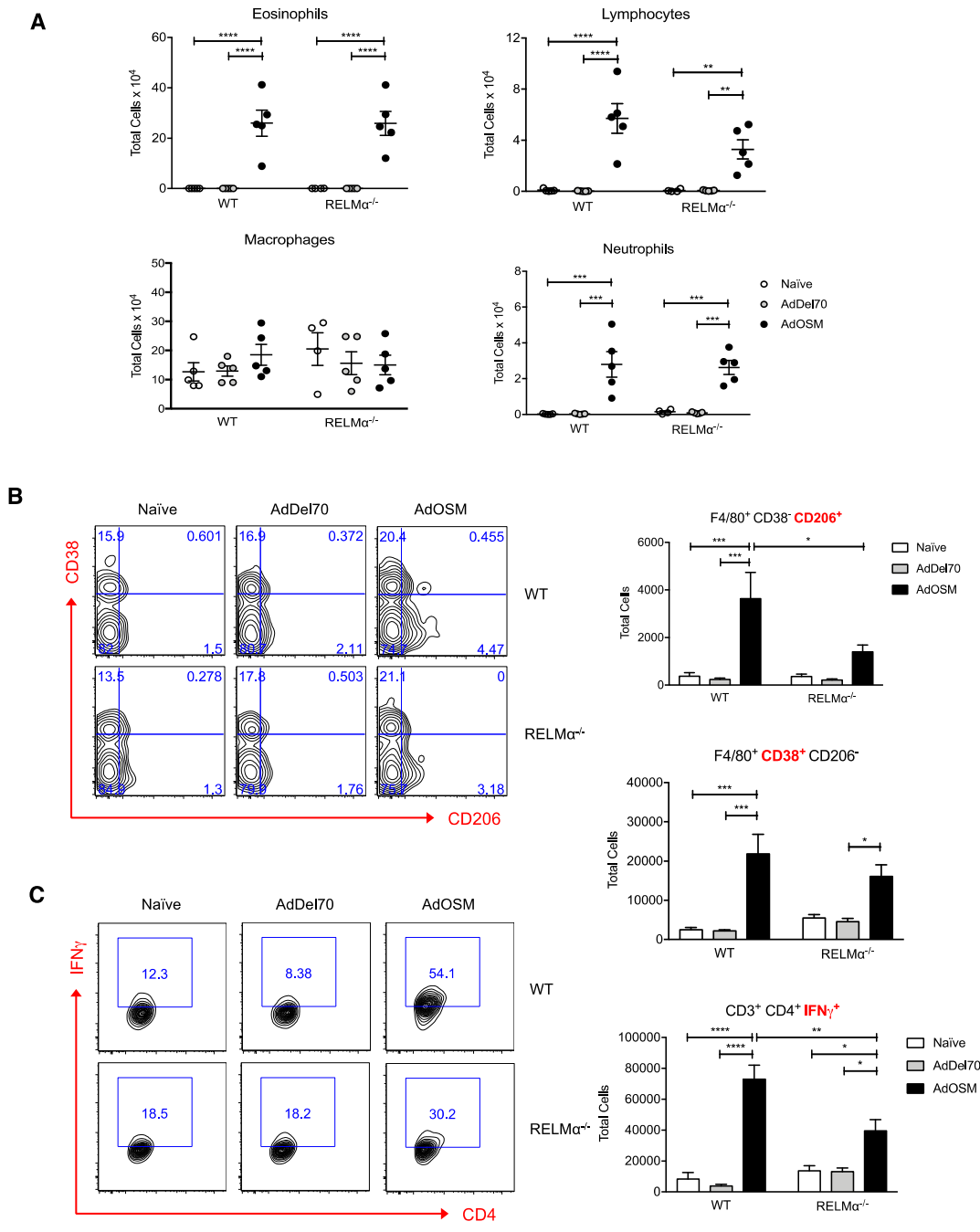


Figure 7. Reduced alternatively activated M2 macrophage numbers in total lung of AdOSM-treated RELM $\alpha^{-/-}$ mice. (A) Enumeration of eosinophils, lymphocytes, macrophages and neutrophils recovered from BAL fluid. (B) Gating strategy (left panel) of F4/80 $^+$ macrophages and total CD38 $^+$ M1 or CD206 $^+$ M2 macrophages (right panel). (C) Gating strategy (left panel) and total IFN γ -producing CD4 $^+$ T cells. Data are represented as mean \pm SEM ($n = 5$ mice/group). Statistical significance was determined by two-way ANOVA with Tukey’s post hoc test (* $p < 0.05$, ** $p < 0.01$, *** $p < 0.001$, **** $p < 0.0001$ between indicated groups).

3.5. RELM α -Deficiency Does Not Alter Th2-Associated Cytokine Elevation but Reduces Arginase1 and Matrix Remodelling Gene Induction

We did not observe significant changes of Th2-associated inflammatory cytokine mRNA expression as a result of RELM α -deficiency (Figure 8A). AdOSM up-regulated similar levels of IL-4, IL-5, IL-6, and IL-33 mRNA after 7 days in both wildtype and RELM $\alpha^{-/-}$ mice (Figure 8A,B). In correlation

with the IFN γ ⁺ Th1 cell population, as assessed by flow cytometry, IFN γ mRNA in total lung was upregulated, albeit to a low extent (2-fold), by AdOSM treatment in wild-type animals, but in RELM α ^{-/-} mice its gene expression was similar across all treatment groups (Figure 8A). In our previous work [22] and here, we could not detect IFN γ protein in BAL fluid. Consistent with our previous findings [22], AdOSM induced Arg1 mRNA, and its expression was significantly reduced in the absence of RELM α (Figure 8B). Together with flow cytometry of CD206⁺ macrophages (Figure 7B), this suggests a potential role for RELM α in maximizing the accumulation of AA/M2 macrophages.

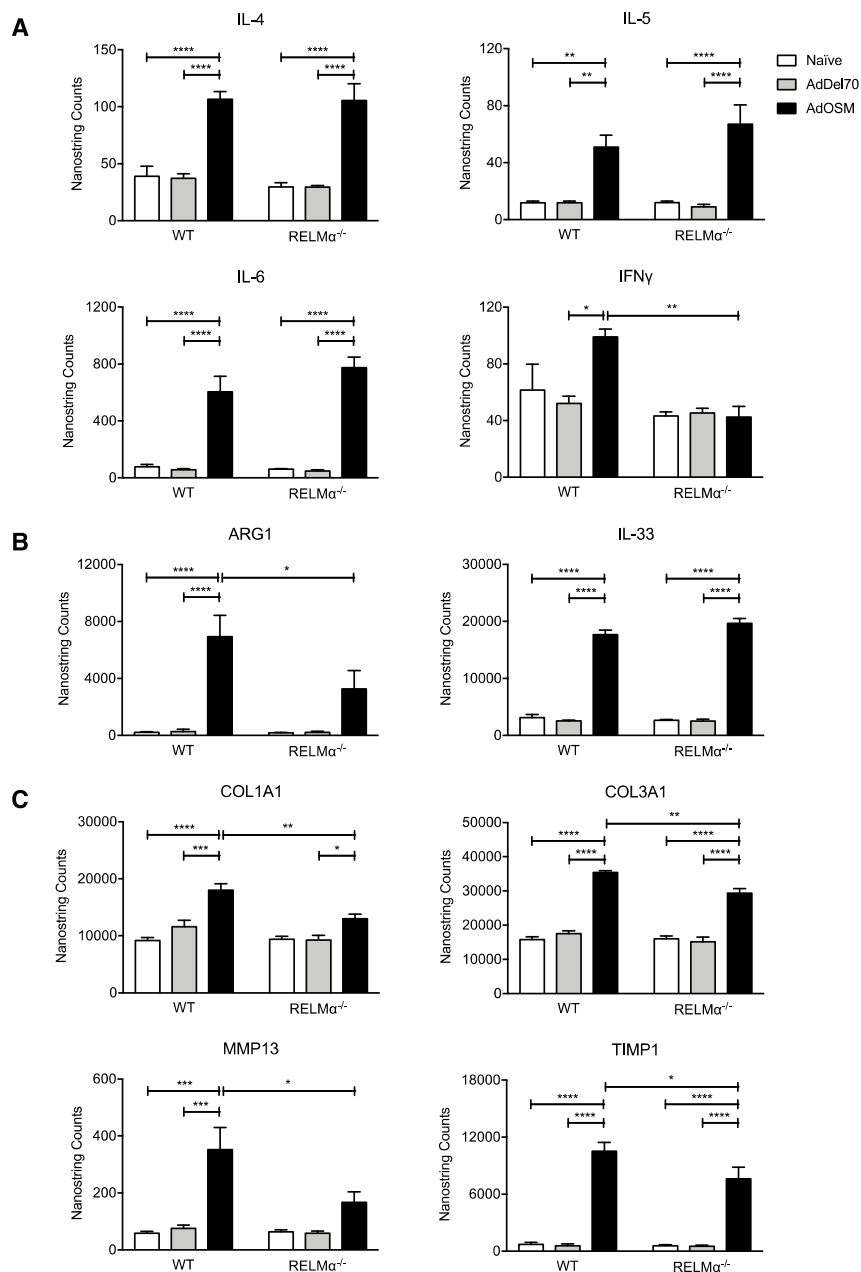


Figure 8. RELM α deficiency modulates mRNA expression of ECM modulating genes, but not Th2-associated inflammatory cytokines. Total lung mRNA expression of (A) inflammatory cytokines, (B) Arg1 and IL-33, and (C) ECM genes. Gene expression levels are represented as NanoString counts and are normalized to housekeeping genes ACTB and PGK1. Data are expressed as mean \pm SEM ($n = 5$ mice/group). Statistical significance was determined by two-way ANOVA with Tukey’s post hoc test (* $p < 0.05$, ** $p < 0.01$, *** $p < 0.001$, **** $p < 0.0001$ between indicated groups).

We have previously demonstrated that pulmonary overexpression of OSM can induce ECM deposition in C57Bl/6 mice [13,36]. We therefore examined the role of RELM α in OSM-induced ECM accumulation by analysis of gene expression. Consistent with our previous findings [13], mRNAs for proteins implicated in ECM remodeling, COL1A1, COL3A1, MMP13, and TIMP1, were up-regulated in lungs of AdOSM-treated wild-type mice at day 7 (Figure 8C). Similar trends were observed in RELM $\alpha^{-/-}$ mice. However the expression of these genes was significantly reduced in the absence of RELM α , suggesting that ECM accumulation induced by OSM may be regulated in part through RELM α .

3.6. RELM α -Deficiency Reduces Cell Proliferation and Parenchymal α SMA Accumulation

Lung tissue sections were examined by histological analyses to determine the effects of RELM α deficiency on cell proliferation, goblet cell hyperplasia, and accumulation of α SMA. Formalin-fixed, paraffin-embedded lung tissue sections stained with H&E showed thickening of the airway epithelium in AdOSM-treated wild-type mouse lungs, which was reduced in RELM α -deficient animals (Figure 9A). These sections were stained with the cell proliferation marker Ki67 to determine whether airway thickness was due to increased proliferating epithelial cells. However, there did not appear to be obvious differences in Ki67⁺ cells in the epithelium between wild-type and RELM $\alpha^{-/-}$ mice at day 7 (Figure 9B). Quantification of Ki67⁺ cells in these sections did show that AdOSM-treated lungs had a greater proportion of Ki67⁺ cells around the airways and throughout the lung parenchyma, whereas in the absence of RELM α there was a significant reduction in proliferating cells (Figure 9E). PAS staining, an indicator of mucous-producing goblet cells, indicated increased numbers of goblet cells in the epithelium of AdOSM-treated mouse lungs, however we did not observe striking differences between wild-type and RELM $\alpha^{-/-}$ animals (Figure 9C). Lung tissues stained for α SMA (Figure 9D) and analysis of entire lung sections, excluding major airways and blood vessels, revealed that AdOSM induced the accumulation of α SMA⁺ cells in the lung parenchyma of wild-type mice (Figure 9F). In RELM $\alpha^{-/-}$ mice treated with AdOSM, there was significantly less α SMA⁺ staining.

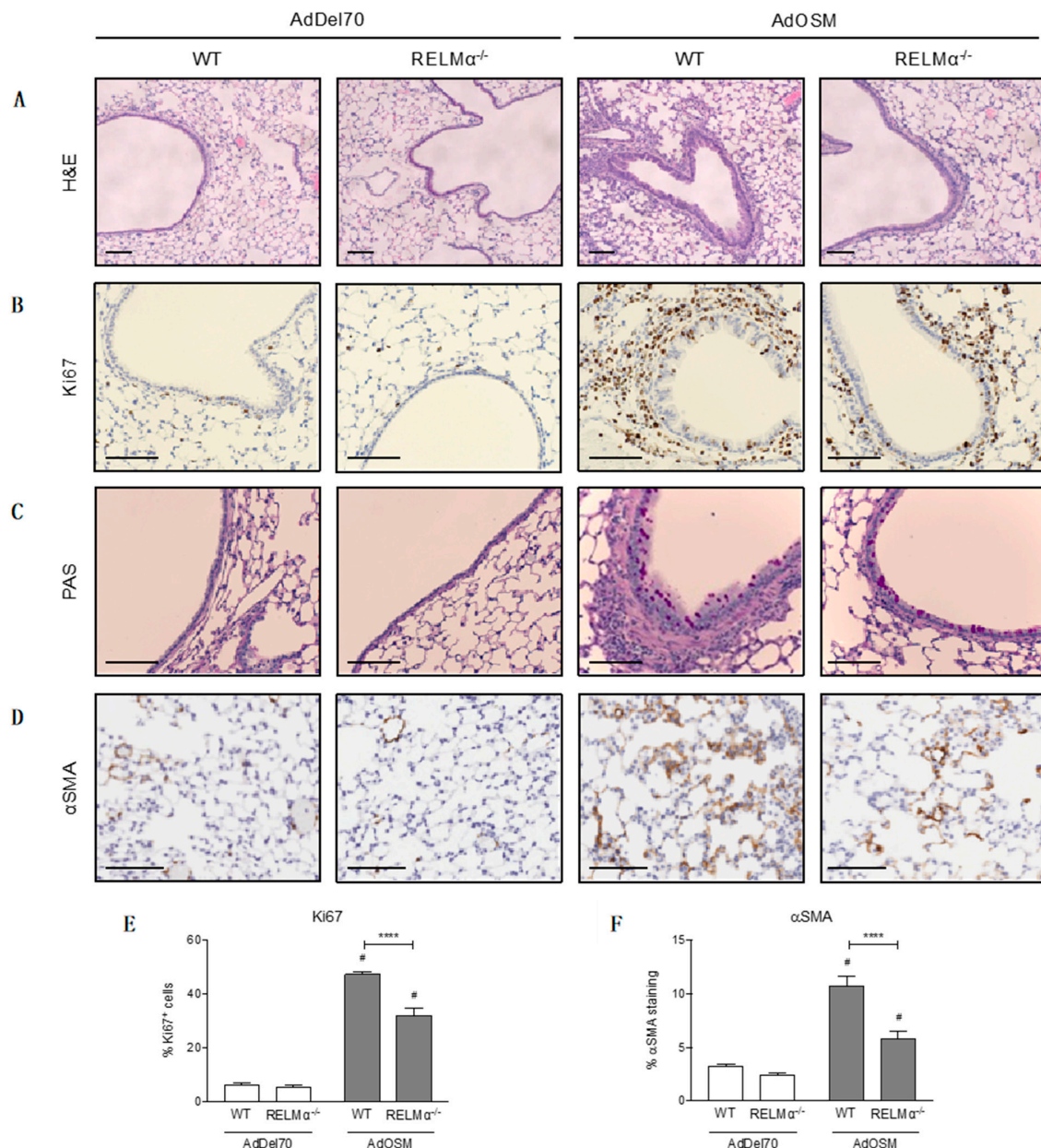


Figure 9. Histological analyses of formalin-fixed, paraffin-embedded lung tissue. Lung sections were prepared from AdDel70- or AdOSM-treated wild-type or RELM $\alpha^{-/-}$ mice as indicated. Representative images of lung tissue sections stained with (A) H&E, (B) Ki67 for proliferating cells, (C) PAS for mucous-producing goblet cells, and (D) α SMA. Scale bars, 100 μ m. (E) Quantification of % Ki67⁺ cells in the epithelium and parenchyma. (F) Quantification of % α SMA staining in the parenchyma per lung tissue section, 3 sections were analyzed per mouse, excluding major airways and blood vessels. Data (E,F) are expressed as mean \pm SEM, # different from AdDel70 ($p < 0.05$). Statistical significance was determined by two-way ANOVA with Tukey's post hoc test (**** $p < 0.0001$ between indicated groups).

4. Discussion

Our results demonstrate that the overexpression of OSM in mouse lungs strongly induces mRNA expression of RELM α in columnar airway epithelial cells (columnar-AEC) and RELM α protein detected in lungs of the C57Bl/6 strain of mice. AEC responded directly to OSM *in vitro*, and OSM-induced RELM α in columnar-AEC did not require STAT6 or IL-6 *in vivo*. OSM also induced YM-1 in whole lung, and YM-1 mRNA in columnar-AEC. This is the first report of gp130 cytokine regulation of RELM α

independently of typical Th2 cytokine environments, and of YM-1 expressed by AEC. Furthermore, RELM α -deficiencies in C57Bl/6 mice did not affect the expression of adenovirus-encoded OSM, nor of mRNA expression of Th2-associated mediators such as IL-4, IL-5, IL-6, and eotaxin-2, nor eosinophil accumulation in BAL fluid. However, the absence of RELM α in deficient mice resulted in less accumulation of AA/M2 macrophages in comparison to wild-type counterparts, less up-regulation of ECM remodeling genes, and less parenchymal α SMA⁺ staining in knockout animals treated with AdOSM, characteristics of altered tissue repair and wound healing phenotypes. This suggests an OSM-RELM α pathway in AEC integrated into tissue healing/repair responses.

Among the gp130 cytokines, the receptor chains for the OSM receptor complex (OSMR β and gp130) are widely expressed on connective tissue cells, and can engage several signaling pathways including JAK/STAT, MAPK, and PI3K/Akt [15,17]. Based on in vitro studies [18,39], OSM is more active than other gp130 cytokines, such as IL-6, LIF, or IL-31, and robustly regulates the expression of signaling intermediates, including STAT3 and STAT1, as well as genes including IL-4R α , IL-6, and ECM genes MMP1 and TIMP1 in connective tissue cells. A similar trend of OSM potency was also observed here in vivo (comparing RELM α and YM-1 response to OSM versus IL-6 over-expression Figures 3A and 5A) and in vitro (comparing pSTAT3 activation, Figure 2C). In lung inflammation with OSM detectable in human disease conditions, OSM may thus engage AEC responses in inflammatory cascades, and although we have shown that human BEAS2B AEC cells respond to OSM in vitro with pSTAT3 activation [13], other endpoints in human airway EC need to be fully explored. OSM is produced by macrophages upon inflammatory stimuli and thus may participate in AEC regulation in TH1-skewed inflammatory environments as well as TH2-skewed local tissue environments.

The use of CISH to determine cellular localization of mRNA signals is useful in examining complex inflammatory models in vivo. Here we show that RELM α was expressed in some CD68⁺ macrophages as expected (presumably AA/M2 macrophages) but in addition CD68⁻ cells in the parenchyma (Figure 2). Others have shown that RELM α can be expressed by alveolar type II epithelial cells using RELM α promoter reporter mice [40]. Thus, alveolar type II epithelial cells may also be responsive to OSM with RELM α expression (we have published that these cells express IL-33 in response to OSM in vitro and in vivo). Our results showing that parenchymal RELM α is lost in STAT6^{-/-} mice suggest that IL-4/13/STAT6 canonical signaling is required for RELM α induction in lung macrophages as previously described [41], but in addition type II alveolar epithelial cells (Figure 4C,D). However, further work is required to explore the STAT6 requirement of Alveolar epithelial cells in this system in vivo. The lack of change in total lung extract RELM α levels may reflect a predominant contribution of airway epithelial cells to total lung RELM α protein load. Parenchymal mRNA signal induction for RELM α was not affected in IL-6^{-/-} mice (Figure 4A,B), suggesting a requirement of STAT6 but not IL-6 in alveolar type II epithelial cell or alveolar macrophage expression of RELM α .

In addition to AEC, YM-1 mRNA was elevated in mononuclear cells in the parenchyma (Figure 5B,C) consistent with AAM/M2 expression of this gene product. IL-6^{-/-} mice showed a decrease in YM-1 total protein (Figure 5A), which is consistent with the ablation of accumulation of Arg1⁺ AAM/M2 cells observed previously in IL-6^{-/-} mice [22]. However, total YM1 was not appreciably ablated in STAT6^{-/-} mice (Figure 5A). YM-1 mRNA was not expressed by alveolar type II cells and thus we suggest that airway epithelial cells contribute significantly to total YM-1 protein levels in this model, supported by the expression of YM-1 mRNA in airway epithelial cells (Figure 5B,C).

RELM α has been implicated in several different murine models of lung inflammation, including parasitic infection and pulmonary fibrosis. In a model of pulmonary inflammation, RELM α ^{-/-} mice challenged with the parasite *Schistosoma mansoni* (*Sm*) eggs presented elevated Th2 cytokine levels including IL-4, IL-5, and IL-13 in comparison to wild-type counterparts [26]. However, in a different model of pulmonary fibrosis where RELM α ^{-/-} mice were treated with bleomycin, these mice exhibited decreased IL-4 expression and less fibrosis in comparison to wild-type mice [33]. In our model of Th2-skewed pulmonary inflammation, Th2 cytokines were not differentially expressed between wild-type and RELM α knockout mice, suggesting the Th2 cell responses were not altered.

We did observe lower IFN γ mRNA expression in RELM $\alpha^{-/-}$ mice (Figure 7A), as well as reduced IFN γ -producing CD4 $^{+}$ Th1 cells in total lung of knockout mice relative to wild-type mice (Figure 6C). However, in this and previous studies [22], we cannot detect IFN γ or IL-12 in BAL fluid, and the mRNA for IFN γ is low and minimally induced (two-fold) by AdOSM in total lung (Figure 8A). That being noted, it appears that RELM α can regulate activated Th1 cells although it is not clear if this is a direct or indirect action. Taken together, the function of RELM α in regulating Th1 and Th2 responses appears dependent on the specific model of lung inflammation.

In a model of type 2 immunity during nematode infection, studies have shown that Ym1 can induce epithelial cell expression of RELM α [42]. Ym1 is another AA/M2 macrophage-associated protein elevated in Th2 inflammation and AdOSM induces Ym1 in our model system in vivo. Whether OSM directly induces RELM α in columnar airway epithelial cells (OSM can directly induce AEC STAT3 signaling), or indirectly through Ym1 (or possibly both pathways), requires further study, since we were not able to detect RELM α production in mouse airway epithelial cells in liquid culture in vitro (data not shown). This may reflect the environment present in vivo (additional factors and/or AEC phenotype) is not recapitulated in in vitro liquid cell culture. It would also be of interest to investigate the expression and potential requirement in inflammation of OSM in *N. brasiliensis* infections, in particular in the lung inflammatory phase, since OSM may participate in the RELM α and Ym1 induction in such nematode infections.

In our system of OSM-induced lung inflammation, although there were no significant differences in Th2 cytokine expression between wild-type and RELM $\alpha^{-/-}$ mice, we did observe a lower fibrotic response in knockout mice treated with AdOSM. Similar to the bleomycin model of pulmonary fibrosis [33], we observed reduced type I collagen lung mRNA expression (Figure 8C), correlating with markedly less α SMA $^{+}$ staining in the lung tissue of RELM $\alpha^{-/-}$ mice relative to wild-type mice (Figure 9F), suggesting that knockout mice were partially protected from this particular fibrotic phenotype, and that RELM α may participate in myofibroblast accumulation. Several studies have suggested a role for AA/M2 macrophages in the exacerbation of pulmonary fibrosis and other models of tissue repair and wound healing [43,44]. Here, we show that AdOSM induced the accumulation of CD206 $^{+}$ M2 macrophages, whereas in the absence of RELM α , there was significantly less accumulation of these macrophages in the lung (Figure 7B). This trend was also associated with reduced lung mRNA expression of ECM remodeling proteins COL1A1, COL3A1, MMP13, and TIMP1 in knockout animals (Figure 8C). Taken together, RELM α may function to maintain M2 macrophage numbers in the lung, which may then contribute to myofibroblast differentiation and ultimately lead to matrix deposition and lung fibrosis.

How RELM α acts on various cells mechanistically is not clear. A receptor for RELM α remains to be fully identified, although some have suggested that RELM α could bind to intracellular Bruton's tyrosine kinase (BTK) [26,45]. While the interaction between the two is unclear since RELM α is secreted whereas BTK is cytoplasmic, activation of the BTK pathway can lead to myeloid cell chemotaxis, and in a different study, down-regulate Th2 cytokine production in CD4 $^{+}$ T cells [26,45]. Others have proposed that RELM α could induce myofibroblast differentiation through the induction of α SMA in fibroblasts [46], however it is unclear how RELM α binds or activates these fibroblasts. RELM α also induces myofibroblast transition of mouse adipocytes and this may play a role in dermal fibrosis [47].

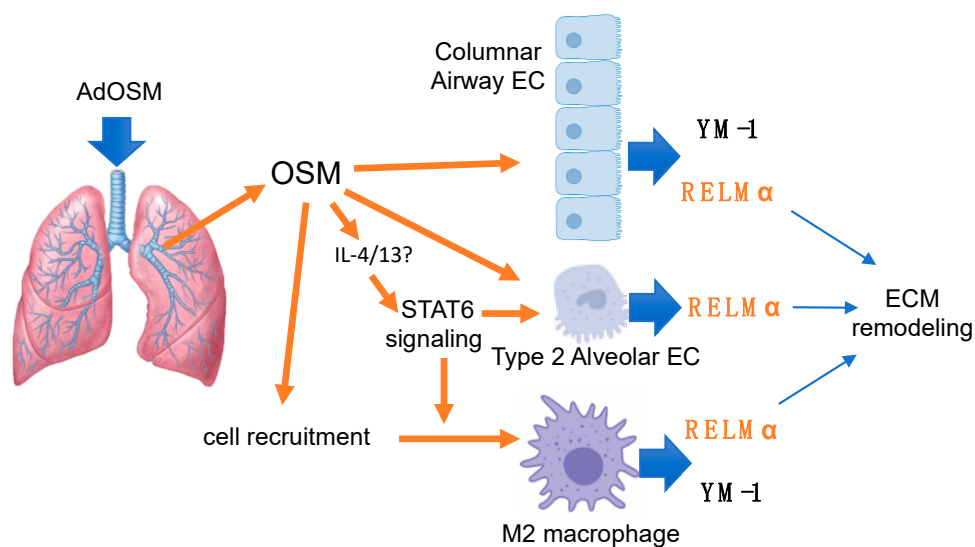
RELM α protein was present basally in serum of naïve mice at approximately 200 ng/mL (Figure 1A), however it is unclear whether RELM α plays a role in systemic circulation in this model. Since the levels of RELM α in BAL fluid can be induced to as high as 12 μ g/mL, it is unlikely that the source of RELM α in lung comes from circulating immune cells, but rather the increase in RELM α levels in serum of AdOSM-treated C57Bl/6 mice is due to spillover or absorption from BAL fluid. Recently, RELM α has been shown implicated in whole-body metabolism in vivo. Kumamoto et al. demonstrated that CD301b $^{+}$ mononuclear phagocytes (MNP) in white adipose tissue were a major source of RELM α [28]. Depletion of these cells disrupted metabolic homeostasis, resulting in significant weight loss and reduced blood glucose levels, and reconstitution of RELM α by intra-peritoneal administration was able

to reestablish glucose homeostasis. Whether the increases of serum RELM α in our system of AdOSM overexpression in C57Bl/6 mice has effects on glucose homeostasis would require further study.

To date, the human homolog for mouse RELM α has yet to be identified. Some have suggested that human RELM β is a functional homologue to mouse RELM α [48]. One study demonstrated that human RELM β was present in epithelial cells and alveolar macrophages of human lung tissue from IPF patients [49], consistent with murine models showing RELM α expression in the same cell types [23]. In another study, RELM β was found at significantly higher levels in bronchial biopsies of patients with asthma compared to healthy individuals and, as the authors suggest, RELM β may play a significant role in airway remodeling mechanisms in human asthma [50]. Further investigation is required to determine whether OSM regulates RELM β in mouse or human lung stromal/epithelial cells.

5. Conclusions

In summary, we have shown that the overexpression of OSM induces a robust expression of RELM α in mouse lungs, induces RELM α in airway epithelial cells without the requirement of IL-6 or STAT6 *in vivo*, and can directly activate airway epithelial cells *in vitro*. RELM α is required in this system for maximal induction of ECM modulating genes, AA/M2 macrophage accumulation and α SMA, but not inflammatory cytokines. These interactions are depicted schematically in the accompanying Scheme 1. Since OSM is elevated in chronic lung diseases in humans, determining the function of the RELM family proteins in OSM-mediated lung inflammation may serve to clarify mechanisms of pathogenesis and/or homeostasis in such conditions.



Scheme 1. AdOSM-induced OSM over-expression in mouse lung elevates RELM α through multiple pathways including: direct activation of columnar airway epithelial cells (EC); indirect activation (STAT6-dependent signaling) putatively in Type 2 alveolar epithelial cells; and also indirectly through recruitment/activation of alternatively activated (M2) macrophages. Matrix remodeling is reduced in RELM $\alpha^{-/-}$ mice.

Supplementary Materials: The following are available online at <http://www.mdpi.com/2073-4409/9/6/1338/s1>, Figure S1: Specificity of anti-murine RELM α polyclonal antibody by Western blot, Figure S2: Murine Tracheal-Bronchial Epithelial (TBE) cells stimulated with gp130-cytokines or IL-4, Figure S3: Control stains (no-probe) in CISH procedure for Figures 4 and 5.

Author Contributions: Conceptualization, F.B. and C.D.R.; Data curation, L.H., A.Y. and F.L.; Formal analysis, L.H., A.Y., F.B. and C.D.R.; Investigation, L.H., A.Y. and F.L.; Methodology, L.H. and F.L.; Project administration, C.D.R.; Resources, C.D.R.; Supervision, F.B. and C.D.R.; Writing—original draft, L.H.; Writing—review & editing, F.B. and C.D.R. All authors have read and agreed to the published version of the manuscript.

Funding: This research was funded by the Canadian Institutes for Health Research (CIHR) operating grant number 137013.

Acknowledgments: We acknowledge expert technical assistance for CISH by Mary Jo Smith from the MIRC Core Histology facility, Jane Ann Smith (in vivo mouse experiments), Bichoy Labib and Dalton Groves (ELISAs), and Rex Park (RT-PCR).

Conflicts of Interest: The authors declare no conflict of interest.

References

1. Burgess, J.K.; Mauad, T.; Tjin, G.; Karlsson, J.C.; Westergren-Thorsson, G. The extracellular matrix—the under-recognized element in lung disease? *J. Pathol.* **2016**, *240*, 397–409. [[CrossRef](#)] [[PubMed](#)]
2. Hogg, P.; Timens, W. The Pathology of Chronic Obstructive Pulmonary Disease. *Annu. Rev. Pathol. Mech. Dis.* **2009**, *4*, 435–459. [[CrossRef](#)] [[PubMed](#)]
3. Mauad, T.; Bel, E.H.; Sterk, P.J. Asthma therapy and airway remodeling. *J. Allergy Clin. Immunol.* **2007**, *120*, 997–1009. [[CrossRef](#)] [[PubMed](#)]
4. King, T.E. Idiopathic Pulmonary Fibrosis: Diagnosis and treatment. International consensus statement. *Am J. Respir Crit Care Med.* **2000**, *161*, 646–664.
5. Wollin, L.; Bonella, F.; Stowasser, S. Idiopathic pulmonary fibrosis: Current treatment options and critical appraisal of nintedanib. *Drug Des. Dev. Ther.* **2015**, *9*, 6407–6419. [[CrossRef](#)] [[PubMed](#)]
6. Re, S.L.; Lison, D.; Huaux, F. CD4+ T lymphocytes in lung fibrosis: Diverse subsets, diverse functions. *J. Leukoc. Boil.* **2013**, *93*, 499–510. [[CrossRef](#)]
7. Wynn, T.A.; Vannella, K.M. Macrophages in Tissue Repair, Regeneration, and Fibrosis. *Immun.* **2016**, *44*, 450–462. [[CrossRef](#)]
8. Bonniaud, P.; Kolb, M.; Galt, T.; Robertson, J.; Robbins, C.; Stampfli, M.; Lavery, C.; Margetts, P.J.; Roberts, A.B.; Gaudie, J. Smad3 Null Mice Develop Airspace Enlargement and Are Resistant to TGF- β -Mediated Pulmonary Fibrosis. *J. Immunol.* **2004**, *173*, 2099–2108. [[CrossRef](#)]
9. Migliaccio, C.T.; Buford, M.C.; Jessop, F.; Holian, A. The IL-4R α pathway in macrophages and its potential role in silica-induced pulmonary fibrosis. *J. Leukoc. Boil.* **2007**, *83*, 630–639. [[CrossRef](#)]
10. Todd, N.W.; Luzina, I.G.; Atamas, S.P. Molecular and cellular mechanisms of pulmonary fibrosis. *Fibrogenesis Tissue Repair* **2012**, *5*, 11. [[CrossRef](#)]
11. Mozaffarian, A.; Brewer, A.W.; Trueblood, E.S.; Luzina, I.G.; Todd, N.W.; Atamas, S.P.; Arnett, H.A. Mechanisms of oncostatin M-induced pulmonary inflammation and fibrosis. *J. Immunol.* **2008**, *181*, 7243–7253. [[CrossRef](#)] [[PubMed](#)]
12. Tanaka, M.; Miyahima, A. Oncostatin M, a multifunctional cytokine. *Rev. Physiol. Biochem. Pharmacol.* **2003**, *149*, 39–52. [[CrossRef](#)] [[PubMed](#)]
13. Wong, S.; Botelho, F.M.; Rodrigues, R.M.; Richards, C. Oncostatin M overexpression induces matrix deposition, STAT3 activation, and SMAD1 Dysregulation in lungs of fibrosis-resistant BALB/c mice. *Lab. Investig.* **2014**, *94*, 1003–1016. [[CrossRef](#)] [[PubMed](#)]
14. O'Donoghue, R.J.J.; Knight, D.A.; Richards, C.; Prele, C.M.; Lau, H.L.; Jarnicki, A.G.; Jones, J.; Bozinovski, S.; Vlahos, R.; Thiem, S.; et al. Genetic partitioning of interleukin-6 signalling in mice dissociates Stat3 from Smad3-mediated lung fibrosis. *EMBO Mol. Med.* **2012**, *4*, 939–951. [[CrossRef](#)]
15. Hermanns, H. Oncostatin M and interleukin-31: Cytokines, receptors, signal transduction and physiology. *Cytokine Growth Factor Rev.* **2015**, *26*, 545–558. [[CrossRef](#)]
16. Richards, C. The Enigmatic Cytokine Oncostatin M and Roles in Disease. *ISRN Inflamm.* **2013**, *2013*, 1–23. [[CrossRef](#)]
17. West, N. Coordination of Immune-Stroma Crosstalk by IL-6 Family Cytokines. *Front. Immunol.* **2019**, *10*, 1093. [[CrossRef](#)]
18. Richards, C.; Izakelian, L.; Dubey, A.; Zhang, G.; Wong, S.; Kwofie, K.; Qureshi, A.; Botelho, F. Regulation of IL-33 by Oncostatin M in Mouse Lung Epithelial Cells. *Mediat. Inflamm.* **2016**, *2016*, 1–12. [[CrossRef](#)]
19. Simpson, J.L.; Baines, K.J.; Boyle, M.J.; Scott, R.J.; Gibson, P.G. Oncostatin M (OSM) is increased in asthma with incompletely reversible airflow obstruction. *Exp. Lung Res.* **2009**, *35*, 781–794. [[CrossRef](#)]
20. Baines, K.J.; Simpson, J.L.; Gibson, P.G. Innate Immune Responses Are Increased in Chronic Obstructive Pulmonary Disease. *PLoS ONE* **2011**, *6*, e18426. [[CrossRef](#)]

21. Pothoven, K.L.; Norton, J.E.; Hulse, K.; Suh, L.A.; Carter, R.G.; Rocci, E.; Harris, K.E.; Shintani-Smith, S.; Conley, D.B.; Chandra, R.K.; et al. Oncostatin M promotes mucosal epithelial barrier dysfunction, and its expression is increased in patients with eosinophilic mucosal disease. *J. Allergy Clin. Immunol.* **2015**, *136*, 737–746. [[CrossRef](#)] [[PubMed](#)]
22. Dubey, A.; Izakelian, L.; A Ayoub, E.; Ho, L.; Stephenson, K.; Wong, S.; Kwofie, K.; Austin, R.C.; Botelho, F.; Ask, K.; et al. Separate roles of IL-6 and oncostatin M in mouse macrophage polarization in vitro and in vivo. *Immunol. Cell Biol.* **2017**, *96*, 257–272. [[CrossRef](#)] [[PubMed](#)]
23. Holcomb, I.N.; Kabakoff, R.C.; Chan, B.; Baker, T.W.; Gurney, A.; Henzel, W.; Nelson, C.; Lowman, H.B.; Wright, B.D.; Skelton, N.J.; et al. FIZZ1, a novel cysteine-rich secreted protein associated with pulmonary inflammation, defines a new gene family. *EMBO J.* **2000**, *19*, 4046–4055. [[CrossRef](#)] [[PubMed](#)]
24. Steppan, C.M.; Brown, E.J.; Wright, C.M.; Bhat, S.; Banerjee, R.R.; Dai, C.Y.; Enders, G.H.; Silberg, D.G.; Wen, X.; Wu, G.D.; et al. A family of tissue-specific resistin-like molecules. *Proc. Natl. Acad. Sci. USA* **2001**, *98*, 502–506. [[CrossRef](#)] [[PubMed](#)]
25. Munitz, A.; Waddell, A.; Seidu, L.; Cole, E.T.; Ahrens, R.; Hogan, S.P.; E Rothenberg, M. Resistin-like molecule α enhances myeloid cell activation and promotes colitis. *J. Allergy Clin. Immunol.* **2008**, *122*, 1200–1207. [[CrossRef](#)]
26. Nair, M.G.; Du, Y.; Perrigoue, J.G.; Zaph, C.; Taylor, J.J.; Goldschmidt, M.; Swain, G.P.; Yancopoulos, G.D.; Valenzuela, D.M.; Murphy, A.J.; et al. Alternatively activated macrophage-derived RELM- α is a negative regulator of type 2 inflammation in the lung. *J. Exp. Med.* **2009**, *206*, 937–952. [[CrossRef](#)]
27. Chen, F.; Wu, W.; Jin, L.; Millman, A.; Palma, M.; El-Naccache, D.; Lothstein, K.E.; Dong, C.; Edelblum, K.L.; Gause, W.C. B Cells Produce the Tissue-Protective Protein RELM α during Helminth Infection, which Inhibits IL-17 Expression and Limits Emphysema. *Cell Rep.* **2018**, *25*, 2775–2783. [[CrossRef](#)]
28. Kumamoto, Y.; Camporez, J.P.G.; Jurczak, M.J.; Shanabrough, M.; Horvath, T.; Shulman, G.I.; Iwasaki, A. CD301b + Mononuclear Phagocytes Maintain Positive Energy Balance through Secretion of Resistin-like Molecule Alpha. *Immun.* **2016**, *45*, 583–596. [[CrossRef](#)]
29. Liu, T.; Jin, H.; Ullenbruch, M.; Hu, B.; Hashimoto, N.; Moore, B.B.; McKenzie, A.; Lukacs, N.W.; Phan, S.H. Regulation of found in inflammatory zone 1 expression in bleomycin-induced lung fibrosis: Role of IL-4/IL-13 and mediation via STAT-6. *J. Immunol.* **2004**, *173*, 3425–3431. [[CrossRef](#)]
30. Nair, M.G.; Cochrane, D.W.; Allen, J.E. Macrophages in chronic type 2 inflammation have a novel phenotype characterized by the abundant expression of Ym1 and Fizz1 that can be partly replicated in vitro. *Immunol. Lett.* **2003**, *85*, 173–180. [[CrossRef](#)]
31. Khorram, N.; Sugimoto, K.; Sheppard, D.; Rosenthal, P.; Cho, J.; Pham, A.; Miller, M.; Zuraw, B.; Croft, M.; Broide, D.; et al. Alternaria Induces Stat-6 Dependent Acute Airway Eosinophilia And Epithelial Fizz1 Expression That Promotes Airway Fibrosis And Epithelial Thickness. *J. Allergy Clin. Immunol.* **2012**, *129*, AB54. [[CrossRef](#)]
32. Lee, M.-R.; Shim, D.; Yoon, J.; Jang, H.S.; Oh, S.-W.; Suh, S.H.; Choi, J.-H.; Oh, G.T. Retnla Overexpression Attenuates Allergic Inflammation of the Airway. *PLoS ONE* **2014**, *9*, e112666. [[CrossRef](#)] [[PubMed](#)]
33. Liu, T.; Yu, H.; Ullenbruch, M.; Jin, H.; Ito, T.; Wu, Z.; Liu, J.; Phan, S.H. The In Vivo Fibrotic Role of FIZZ1 in Pulmonary Fibrosis. *PLoS ONE* **2014**, *9*, e88362. [[CrossRef](#)] [[PubMed](#)]
34. Knipper, J.A.; Willenborg, S.; Brinckmann, J.; Bloch, W.; Maaß, T.; Wagener, R.; Krieg, T.; Sutherland, T.E.; Munitz, A.; Rothenberg, M.E.; et al. Interleukin-4 Receptor α Signaling in Myeloid Cells Controls Collagen Fibril Assembly in Skin Repair. *Immun.* **2015**, *43*, 803–816. [[CrossRef](#)]
35. Chen, G.; Wang, S.H.; Jang, J.; Odegaard, J.I.; Nair, M.G. Comparison of RELM α and RELM β Single- and Double-Gene-Deficient Mice Reveals that RELM α Expression Dictates Inflammation and Worm Expulsion in Hookworm Infection. *Infect. Immun.* **2016**, *84*, 1100–1111. [[CrossRef](#)]
36. Fritz, D.K.; Kerr, C.; Fattouh, R.; Llop-Guevara, A.; Khan, W.I.; Jordana, M.; Richards, C. A Mouse Model of Airway Disease: Oncostatin M-Induced Pulmonary Eosinophilia, Goblet Cell Hyperplasia, and Airway Hyperresponsiveness Are STAT6 Dependent, and Interstitial Pulmonary Fibrosis Is STAT6 Independent. *J. Immunol.* **2010**, *186*, 1107–1118. [[CrossRef](#)]
37. Botelho, F.M.; Rangel-Moreno, J.; Fritz, D.; Randall, T.D.; Xing, Z.; Richards, C. Pulmonary expression of oncostatin M (OSM) promotes inducible BALT formation independently of IL-6, despite a role for IL-6 in OSM-driven pulmonary inflammation. *J. Immunol.* **2013**, *191*, 1453–1464. [[CrossRef](#)]

38. Munitz, A.; Cole, E.T.; Karo-Atar, D.; Finkelman, F.D.; E Rothenberg, M. Resistin-Like Molecule- α Regulates IL-13-Induced Chemokine Production but Not Allergen-Induced Airway Responses. *Am. J. Respir. Cell Mol. Biol.* **2012**, *46*, 703–713. [[CrossRef](#)]
39. Fritz, D.K.; Kerr, C.; Botelho, F.; Stampfli, M.; Richards, C. Oncostatin M (OSM) primes IL-13- and IL-4-induced eotaxin responses in fibroblasts: Regulation of the type-II IL-4 receptor chains IL-4R α and IL-13R α 1. *Exp. Cell Res.* **2009**, *315*, 3486–3499. [[CrossRef](#)]
40. Krljanac, B.; Schubart, C.; Naumann, R.; Wirtz, S.; Culemann, S.; Krönke, G.; Voehringer, D. RELMa-expressing macrophages protect against fatal lung damage and reduce parasite burden during helminth infection. *Sci. Immunol.* **2019**, *4*, 1–11. [[CrossRef](#)]
41. Stütz, A.M.; Pickart, L.A.; Trifilieff, A.; Baumruker, T.; Prieschl-Strassmayr, E.; Woisetschläger, M. The Th2 Cell Cytokines IL-4 and IL-13 Regulate Found in Inflammatory Zone 1/Resistin-Like Molecule Gene Expression by a STAT6 and CCAAT/Enhancer-Binding Protein-Dependent Mechanism. *J. Immunol.* **2003**, *170*, 1789–1796. [[CrossRef](#)]
42. Sutherland, T.E.; Rückerl, D.; Logan, N.; Duncan, S.; Wynn, T.A.; Allen, J.E. Ym1 induces RELM α and rescues IL-4R α deficiency in lung repair during nematode infection. *PLoS Pathog.* **2018**, *14*, e1007423. [[CrossRef](#)]
43. Ayaub, E.A.; Dubey, A.; Imani, J.; Botelho, F.; Kolb, M.R.J.; Richards, C.; Ask, K. Overexpression of OSM and IL-6 impacts the polarization of pro-fibrotic macrophages and the development of bleomycin-induced lung fibrosis. *Sci. Rep.* **2017**, *7*, 13281. [[CrossRef](#)] [[PubMed](#)]
44. Gibbons, M.A.; MacKinnon, A.C.; Ramachandran, P.; Dhaliwal, K.; Duffin, R.; Phythian-Adams, A.; Van Rooijen, N.; Haslett, C.; Howie, S.E.M.; Simpson, A.J.; et al. Ly6C hi Monocytes Direct Alternatively Activated Profibrotic Macrophage Regulation of Lung Fibrosis. *Am. J. Respir. Crit. Care Med.* **2011**, *184*, 569–581. [[CrossRef](#)] [[PubMed](#)]
45. Su, Q.; Zhou, Y.; Johns, R.A. Bruton's tyrosine kinase (BTK) is a binding partner for hypoxia induced mitogenic factor (HIMF/FIZZ1) and mediates myeloid cell chemotaxis. *FASEB J.* **2007**, *21*, 1376–1382. [[CrossRef](#)]
46. Liu, T.; Hu, B.; Choi, Y.Y.; Chung, M.; Ullenbruch, M.; Yu, H.; Lowe, J.B.; Phan, S.H. Notch1 Signaling in FIZZ1 Induction of Myofibroblast Differentiation. *Am. J. Pathol.* **2009**, *174*, 1745–1755. [[CrossRef](#)]
47. Martins, V.; Santos, F.G.D.L.; Wu, Z.; Capelozzi, V.; Phan, S.H.; Liu, T. FIZZ1-induced myofibroblast transdifferentiation from adipocytes and its potential role in dermal fibrosis and lipoatrophy. *Am. J. Pathol.* **2015**, *185*, 2768–2776. [[CrossRef](#)]
48. Pine, G.M.; Batugedara, H.; Nair, M. Here, there and everywhere: Resistin-like molecules in infection, inflammation, and metabolic disorders. *Cytokine* **2018**, *110*, 442–451. [[CrossRef](#)] [[PubMed](#)]
49. Liu, T.; Baek, H.A.; Yu, H.; Lee, H.J.; Park, B.H.; Ullenbruch, M.; Liu, J.; Nakashima, T.; Choi, Y.Y.; Wu, G.D.; et al. FIZZ2/RELM- β Induction and Role in Pulmonary Fibrosis. *J. Immunol.* **2011**, *187*, 450–461. [[CrossRef](#)] [[PubMed](#)]
50. Fang, C.L.; Yin, L.J.; Sharma, S.; Kierstein, S.; Wu, H.F.; Eid, G.; Haczku, A.; Corrigan, C.J.; Ying, S. Resistin-like molecule- β (RELM- β) targets airways fibroblasts to effect remodelling in asthma: From mouse to man. *Clin. Exp. Allergy* **2015**, *45*, 940–952. [[CrossRef](#)] [[PubMed](#)]

